STABILITY AND CHAOS IN HAMILTONIAN SYSTEMS: FROM LOCAL TO GLOBAL DYNAMICS

Tassos BOUNTIS

Haris SKOKOS and Christos ANTONOPOULOS

First Mediterranean Conference on Nonlinear Dynamics and its Applications

Pescara, Italy, July 3 - 8, 2008

Lecture 2

The GALI$_k$ Indices: A Geometrical Study of the Dynamics of Hamiltonian Systems

Department of Mathematics and Center for Research and Applications of Nonlinear Systems (CRANS), University of Patras, GR–26500, Rion, Patras, Greece

Contents

1. A Brief Review of the SALI Method
2. GALI$_k(t)$: Chaos and Order in Multidimensions
3. Analytical Estimates for the GALI$_k(t)$ Indices
4. Numerical Verification and Applications
5. Dimensionality of Tori and Weak Diffusion
6. Conclusions

Geometric Interpretation of the SALI

We note that the SALI may be equivalently evaluated using the 'wedge' product of the two **deviation unit vectors** $\hat{w}_1 \wedge \hat{w}_1$ for which it holds

$$\|\hat{w}_1 \wedge \hat{w}_2\| = \frac{\|\hat{w}_1 - \hat{w}_2\| \cdot \|\hat{w}_1 + \hat{w}_2\|}{2} \quad . \tag{1}$$

Thus, the SALI is related to **the 'area' between the 2 deviation vectors**, $\hat{w}_1$, $\hat{w}_2$.
Generalizing to more than two deviations $\hat{w}_1, \hat{w}_2, \ldots, \hat{w}_k$, $2 \leq k \leq 2N$, we introduce an index that is proportional to **the 'volume' of the parallelepiped** that has these vectors as vertices.
All normalized deviation vectors $\hat{w}_i$, $i = 1, 2, \ldots, 2N$, can be written as

$$\hat{w}_i = \sum_{j=1}^{2N} w_{ij} \hat{e}_j \quad , \quad i = 1, 2, \ldots, k \tag{2}$$

when expressed in terms of the usual orthonormal basis of the n–dimensional Euclidian space.

The wedge product of these k deviation vectors can be written with respect to the basis $\hat{e}_{i_k}$

$$\hat{w}_1 \wedge \hat{w}_2 \wedge \cdots \wedge \hat{w}_k = \sum_{1 \le i_1 < i_2 < \cdots < i_k \le 2N} \begin{vmatrix} w_{1i_1} & w_{1i_2} & \cdots & w_{1i_k} \\ w_{2i_1} & w_{2i_2} & \cdots & w_{2i_k} \\ \vdots & \vdots & & \vdots \\ w_{ki_1} & w_{ki_2} & \cdots & w_{ki_k} \end{vmatrix} \hat{e}_{i_1} \wedge \hat{e}_{i_2} \wedge \cdots \wedge \hat{e}_{i_k} \quad (3)$$

If **at least two** of the normalized deviation vectors $\hat{w}_i$, $i = 1, 2, \ldots, k$ are **linearly dependent**, all the $k \times k$ determinants will become zero **making the 'volume' vanish**. We define the norm of this quantity, $\|\hat{w}_1(t) \wedge \hat{w}_2(t) \wedge \cdots \wedge \hat{w}_k(t)\|$, as the generalized index

$$GALI_k(t) = \left\{ \sum_{1 \le i_1 < i_2 < \cdots < i_k \le 2N} \begin{vmatrix} w_{1i_1} & w_{1i_2} & \cdots & w_{1i_k} \\ w_{2i_1} & w_{2i_2} & \cdots & w_{2i_k} \\ \vdots & \vdots & & \vdots \\ w_{ki_1} & w_{ki_2} & \cdots & w_{ki_k} \end{vmatrix}^2 \right\}^{1/2} \quad (4)$$

Analytical Estimates for the GALI$_k(t)$ Indices

If at least one of the deviation vectors **becomes linearly dependent** on the remaining ones, GALI$_k(t)$ will tend to zero as the volume of the parallelepiped having the vectors $\hat{w}_i$ as edges shrinks to zero. On the other hand, if GALI$_k(t)$ remains far from zero, this would indicate the **linear independence** of the deviation vectors.

Theoretical results for the Time Evolution of GALI

Exponential decay of GALI for chaotic orbits

Let us first investigate the dynamics in the vicinity of a chaotic orbit of the Hamiltonian system, with N degrees of freedom. Let $\lambda_1 \geq \lambda_2 \geq \cdots \geq \lambda_{2N}$ be the 'local Lyapunov exponents' oscillating about their time averaged values

$$\sigma_1 \geq \sigma_2 \geq \cdots \geq \sigma_{N-1} \geq \sigma_N = \sigma_{N+1} = 0 \geq \sigma_{N+2} \geq \cdots \geq \sigma_{2N}. \quad (5)$$

which are the 'global' LCEs. Assuming that the λ_i, $i = 1, 2, \ldots, 2N$ do not fluctuate significatively, the evolution of any initial deviation vector $\vec{w}_i$ may be written as

$$\vec{w}_i(t) = \sum_{j=1}^{2N} c_j^i \, e^{\sigma_j t} \, \hat{u}_j \, , \quad (6)$$

A leading order estimate of the deviation vector's Euclidean norm, for long enough times, is

$$\|\vec{w}_i(t)\| \approx |c_1^i| e^{\sigma_1 t} \, . \tag{7}$$

Note that the quantity

$$S_k = \left\{ \sum_{1 \le i_1 < i_2 < \cdots < i_k \le 2N} \left| \begin{array}{cccc} c_{1 i_1} & c_{1 i_2} & \cdots & c_{1 i_k} \\ c_{2 i_1} & c_{2 i_2} & \cdots & c_{2 i_k} \\ \vdots & \vdots & & \vdots \\ c_{k i_1} & c_{k i_2} & \cdots & c_{k i_k} \end{array} \right|^2 \right\}^{1/2} \tag{8}$$

is *not identical* with the norm of the original GALI$_k$, as the wedge product here is not expressed with respect to the usual basis. Thus one should consider the transformation

$$\left[\begin{array}{cccc} \hat{u}_1 & \hat{u}_2 & \ldots & \hat{u}_{2N} \end{array} \right]^{\mathrm{T}} = \mathbf{T}_c \cdot \left[\begin{array}{cccc} \hat{e}_1 & \hat{e}_2 & \ldots & \hat{e}_{2N} \end{array} \right]^{\mathrm{T}} , \tag{9}$$

between the two bases, with $\mathbf{T}_c$ denoting the transformation matrix.

The determinants appearing in the definition of S_k (see equation (**??**)) can be divided in two categories depending on whether they contain or not the first column of matrix **C**. Using standard properties of determinants, we see that those that do contain the first column yield

$$D_{1,j_1,j_2,\ldots,j_{k-1}} = \begin{vmatrix} s_1 & \frac{c^1_{j_1}}{|c^1_1|}e^{-(\sigma_1-\sigma_{j_1})t} & \cdots & \frac{c^1_{j_{k-1}}}{|c^1_1|}e^{-(\sigma_1-\sigma_{j_{k-1}})t} \\ s_2 & \frac{c^2_{j_1}}{|c^2_1|}e^{-(\sigma_1-\sigma_{j_1})t} & \cdots & \frac{c^2_{j_{k-1}}}{|c^2_1|}e^{-(\sigma_1-\sigma_{j_{k-1}})t} \\ \vdots & \vdots & & \vdots \\ s_k & \frac{c^k_{j_1}}{|c^k_1|}e^{-(\sigma_1-\sigma_{j_1})t} & \cdots & \frac{c^k_{j_{k-1}}}{|c^k_1|}e^{-(\sigma_1-\sigma_{j_{k-1}})t} \end{vmatrix} =$$

$$= \begin{vmatrix} s_1 & \frac{c^1_{j_1}}{|c^1_1|} & \cdots & \frac{c^1_{j_{k-1}}}{|c^1_1|} \\ s_2 & \frac{c^2_{j_1}}{|c^2_1|} & \cdots & \frac{c^2_{j_{k-1}}}{|c^2_1|} \\ \vdots & \vdots & & \vdots \\ s_k & \frac{c^k_{j_1}}{|c^k_1|} & \cdots & \frac{c^k_{j_{k-1}}}{|c^k_1|}. \end{vmatrix} e^{-\left[(\sigma_1-\sigma_{j_1})+(\sigma_1-\sigma_{j_2})+\cdots+(\sigma_1-\sigma_{j_{k-1}})\right]t} \qquad (10)$$

Thus, the time evolution of $D_{1,j_1,j_2,\ldots,j_{k-1}}$ is mainly determined by the exponential law

$$D_{1,j_1,j_2,\ldots,j_{k-1}} \propto e^{-\left[(\sigma_1-\sigma_{j_1})+(\sigma_1-\sigma_{j_2})+\cdots+(\sigma_1-\sigma_{j_{k-1}})\right]t} . \quad (11)$$

The determinants that do *not* contain the first column of the transformation matrix tend to zero following an exponential law that decays faster.
Clearly, from all determinants the one that decreases the *slowest* is the one containing the first k columns of matrix **C**, yielding the approximation that GALI$_k$ tends to zero as

$$\text{GALI}_k(t) \propto e^{-[(\sigma_1-\sigma_2)+(\sigma_1-\sigma_3)+\cdots+(\sigma_1-\sigma_k)]t} . \quad (12)$$

The evaluation of GALI for ordered orbits

As is well–known, ordered orbits typically lie on N–dimensional tori, which can be described by a local transformation to action–angle variables, locally satisfying

$$\begin{aligned} \dot{J}_i &= 0 \\ \dot{\theta}_i &= \omega_i(J_1, J_2, \ldots, J_N) \end{aligned} \qquad i = 1, 2, \ldots, N. \tag{13}$$

These can be easily integrated to give

$$\begin{aligned} J_i(t) &= J_{i0} \\ \theta_i(t) &= \theta_{i0} + \omega_i(J_{10}, J_{20}, \ldots, J_{N0})\, t \end{aligned} \qquad i = 1, 2, \ldots, N, \tag{14}$$

By denoting as ξ_i, η_i, $i = 1, 2, \ldots, N$ small deviations of J_i and θ_i respectively, the variational equations of system (**??**), can be solved to yield:

$$\begin{aligned} \xi_i(t) &= \xi_i(0) \\ \eta_i(t) &= \eta_i(0) + \left[\sum_{j=1}^{N} \omega_{ij}\xi_j(0)\right]\, t \end{aligned} \qquad i = 1, 2, \ldots, N. \tag{15}$$

This implies a linear increase of the norm of the deviation vector

$$\|\vec{w}(t)\| = \left\{ 1 + \left[\sum_{i=1}^{N} \left(\sum_{j=1}^{N} \omega_{ij} \xi_j(0) \right) \right] t^2 + \left[2 \sum_{i=1}^{N} \left(\eta_i(0) \sum_{j=1}^{N} \omega_{ij} \xi_j(0) \right) \right] t \right\}^{1/2}, \quad (16)$$

Therefore, the normalized deviation vector tends to **fall on the tangent space of the torus**, since its coordinates perpendicular to the torus (i. e. the coordinates along the action directions) vanish following a t^{-1} rate.

Let us now study the case of k, general, linearly independent unit deviation vectors $\{\hat{w}_1, \hat{w}_2, \ldots, \hat{w}_k\}$ with $2 \leq k \leq 2N$. Using as vector basis the set $\{\hat{v}_1, \hat{v}_2, \ldots, \hat{v}_{2N}\}$ we get:

$$\left[\begin{array}{cccc} \hat{w}_1 & \hat{w}_2 & \ldots & \hat{w}_k \end{array} \right]^{\mathrm{T}} = \mathbf{D} \cdot \left[\begin{array}{cccc} \hat{v}_1 & \hat{v}_2 & \ldots & \hat{v}_{2N} \end{array} \right]^{\mathrm{T}} \quad (17)$$

If *no* deviation vector is initially located in the tangent space of the torus, matrix **D** has the form

$$\mathbf{D} = [d_{ij}] = \frac{1}{\prod_{m=1}^{k} \|\vec{w}_m(t)\|} \cdot \mathbf{D}^{0,k}(t). \quad (18)$$

where $i = 1, 2, \ldots, k$ and $j = 1, 2, \ldots, 2N$. Recalling our earlier discussion, the norm of vector $\vec{w}_i(t)$ for long times, grows linearly with t as

$$M_i(t) = \|\vec{w}_i(t)\| \propto t. \tag{19}$$

the matrix **D** assumes the much simpler form

$$\mathbf{D}(t) = \frac{1}{t^k} \cdot \mathbf{D}^k(t). \tag{20}$$

The Case of N-Dimensional Tori

If k is lower than the dimension of the tangent space of the torus, i. e. $2 \leq k \leq N$, the fastest increasing determinants in this case are $\propto t^k$. Thus, we conclude that the contribution to the behavior of $GALI_k$ is to provide constant terms.
All other determinants introduce terms that grow at a rate **slower** than t^k, proportional to $t^{k-m}/t^k = 1/t^m$. So we arrive at the important result

$$\text{GALI}_k(t) \approx \text{constant} \;\; \text{for} \;\; 2 \leq k \leq N. \tag{21}$$

In the important case of $N < k \leq 2N$ deviation vectors, the fastest growing determinants have the time evolution

$$Determinants \propto t^{2N-k}. \tag{22}$$

and contribute to the time evolution of $GALI_k$ terms proportional to

$$\text{GALI}_k(t) \propto t^{2N-k}/t^k = 1/t^{2(k-N)}. \tag{23}$$

All other determinants introduce terms that tend to zero faster than $1/t^{2(k-N)}$.

The Case of Tori with Dimension Lower than N

In the case of an s–dimensional torus, the k deviation vectors eventually fall on its s–dimensional tangent space spanned by $\hat{v}_{N+1}, \ldots, \hat{v}_{N+s}$. If we start with $2 \leq k \leq s$ deviation vectors, the GALI$_k$ indices will oscillate about **a nonzero constant**. However, for $s < k \leq 2N$ deviation vectors, some of them will become linearly dependent and the GALI$_k$ will **tend to zero by a power law**.

Let us first turn to the case of $s < k \leq 2N - s$. The fastest growing determinants are those containing the s columns of the matrix $\mathbf{D}^k$ with $\omega_{ij} \neq 0$, having as many columns proportional to t as possible. Since t appears at most s times and GALI$_k$ is proportional to $t^s/t^k = 1/t^{(k-s)}$, we conclude that GALI$_k(t) \sim t^{(s-k)}$ for $s < k \leq 2N - s$.
Finally, we consider the behavior of GALI$_k$ when $2N - s < k \leq 2N$. The fastest growing determinants here have t appearing $2N - k$ times and the GALI$_k$ is proportional to $t^{2N-k}/t^k = 1/t^{2(k-N)}$.
In conclusion, we have shown that for chaotic orbits:

$$\text{GALI}_k(t) \propto e^{-[(\sigma_1-\sigma_2)+(\sigma_1-\sigma_3)+\cdots+(\sigma_1-\sigma_k)]t} . \tag{24}$$

while for regular orbits lying on an s–dimensional torus behave as:

$$\text{GALI}_k(t) \sim \begin{cases} \text{constant} & \text{if } 2 \leq k \leq s \\ \frac{1}{t^{k-s}} & \text{if } s < k \leq 2N - s \\ \frac{1}{t^{2(k-N)}} & \text{if } 2N - s < k \leq 2N \end{cases} . \tag{25}$$

Note that from (**??**) we deduce that for $s = N$, GALI$_k$ remains constant for $2 \leq k \leq N$ and decreases to zero as $\sim 1/t^{2(k-N)}$ for $N < k \leq 2N$.

GALI$_k(t)$: Numerical Computations and the SVD Approach

We can write equations (**??**) in matrix form as:

$$\begin{bmatrix} \hat{w}_1 \\ \hat{w}_2 \\ \vdots \\ \hat{w}_k \end{bmatrix} = \begin{bmatrix} w_{11} & w_{12} & \cdots & w_{1\,2N} \\ w_{21} & w_{22} & \cdots & w_{2\,2N} \\ \vdots & \vdots & & \vdots \\ w_{k1} & w_{k2} & \cdots & w_{k\,2N} \end{bmatrix} \cdot \begin{bmatrix} \hat{e}_1 \\ \hat{e}_2 \\ \vdots \\ \hat{e}_{2N} \end{bmatrix} = \mathbf{A} \cdot \begin{bmatrix} \hat{e}_1 \\ \hat{e}_2 \\ \vdots \\ \hat{e}_{2N} \end{bmatrix} . \qquad (26)$$

Since GALI$_k$ measures the volume of the k–parallelepiped P_k having as edges the k unitary deviation vectors $\hat{w}_i$, $i = 1, \ldots, k$, given by:

$$\text{vol}(P_k) = \sqrt{\det(\mathbf{A} \cdot \mathbf{A}^{\mathrm{T}})} \ , \qquad (27)$$

(where $(^{\mathrm{T}})$ denotes transpose), we finally have:

$$\text{GALI}_k = \sqrt{\det(\mathbf{A} \cdot \mathbf{A}^{\mathrm{T}})}, \qquad (28)$$

where only the multiplication of two matrices and the square root of one determinant appears.

Thus we can avoid the computation of many determinants and evaluate GALI$_k$ by performing the Singular Value Decomposition (SVD) of $\mathbf{A}^{\mathrm{T}}$ as follows: The $2N \times k$ matrix $\mathbf{A}^{\mathrm{T}}$ is written as the product of a $2N \times k$ column–orthogonal matrix **U**, a $k \times k$ diagonal matrix **Z** with elements z_i, $i = 1, \ldots, k$ (the so–called *singular values*), and the transpose of a $k \times k$ orthogonal matrix **V**:

$$\mathbf{A}^{\mathrm{T}} = \mathbf{U} \cdot \mathbf{Z} \cdot \mathbf{V}^{\mathrm{T}}. \tag{29}$$

We note that matrices **U** and **V** are orthogonal so that:

$$\mathbf{U}^{\mathrm{T}} \cdot \mathbf{U} = \mathbf{V}^{\mathrm{T}} \cdot \mathbf{V} = \mathrm{I}_k, \tag{30}$$

I_k being the $k \times k$ unit matrix. Using Eq. (**??**) for the computation of GALI$_k$, as well as Eqs. (**??**) and (**??**), we get:

$$\begin{aligned} \mathrm{GALI}_k &= \sqrt{\det\left(\mathbf{A} \cdot \mathbf{A}^{\mathrm{T}}\right)} = \sqrt{\det\left(\mathbf{V} \cdot \mathbf{Z}^{\mathrm{T}} \cdot \mathbf{U}^{\mathrm{T}} \cdot \mathbf{U} \cdot \mathbf{Z} \cdot \mathbf{V}^{\mathrm{T}}\right)} \\ &= \sqrt{\det\left(\mathbf{V} \cdot \mathrm{diag}(z_i^2) \cdot \mathbf{V}^{\mathrm{T}}\right)} = \sqrt{\det\left(\mathrm{diag}(z_i^2)\right)} = \prod_{i=1}^{k} z_i \, . \end{aligned}$$

Numerical verification and applications

We shall use two examples with 2 (2D) and 3 (3D) degrees of freedom: the 2D Hénon–Heiles Hamiltonian

$$H_2 = \frac{1}{2}(p_x^2 + p_y^2) + \frac{1}{2}(x^2 + y^2) + x^2 y - \frac{1}{3}y^3, \tag{31}$$

and the 3D Hamiltonian system:

$$H_3 = \sum_{i=1}^{3} \frac{\omega_i}{2}(q_i^2 + p_i^2) + q_1^2 q_2 + q_1^2 q_3, \tag{32}$$

for the parameters $H_2 = 0.125$ and $H_3 = 0.09$, with $\omega_1 = 1$, $\omega_2 = \sqrt{2}$ and $\omega_3 = \sqrt{3}$.

A 2D Hamiltonian system

Let us consider first a chaotic orbit of the 2D Hamiltonian (**??**), with initial conditions $x = 0$, $y = -0.25$, $p_x = 0.42$, $p_y = 0$. In the figure below, we see the time evolution of $L_1(t)$ of this orbit, which is a good approximation of the maximal LCE, σ_1. Actually, for $t \approx 10^5$, we find $\sigma_1 \approx 0.047$.

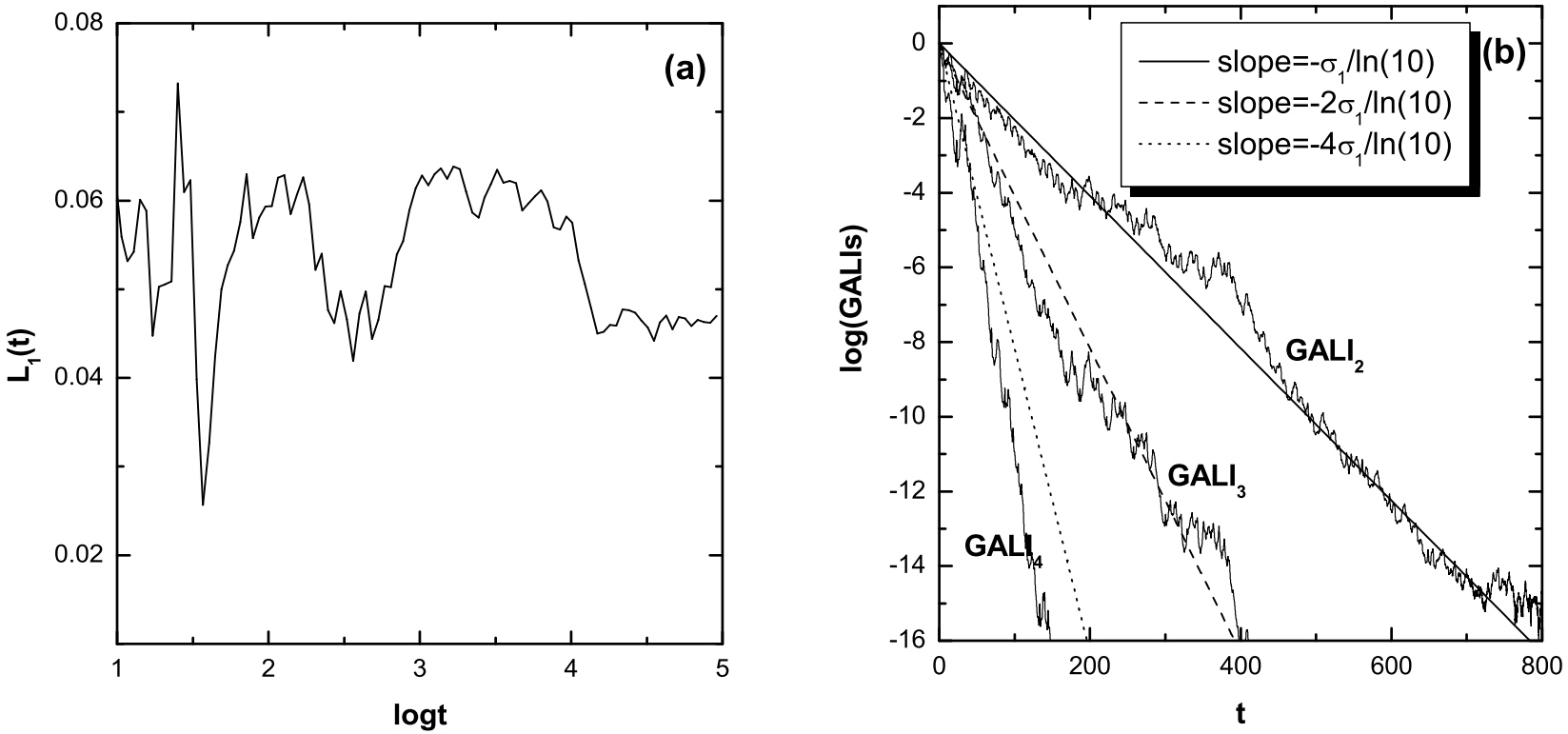

Figure 11:(a) $L_1(t)$ for a chaotic orbit of the 2D system. (b) The evolution of GALI$_2$, GALI$_3$ and GALI$_4$ for the same orbit. We find $\sigma_1 \approx 0.047$, and we know $\sigma_2 = 0$ and $\sigma_3 = -\sigma_2$ and $\sigma_4 = -\sigma_1$. So, GALI$_k$ behaves as

$$\text{GALI}_2(t) \propto e^{-\sigma_1 t}, \;\; \text{GALI}_3(t) \propto e^{-2\sigma_1 t}, \;\; \text{GALI}_4(t) \propto e^{-4\sigma_1 t}. \qquad (33)$$

Now, for an ordered orbit of our 2D Hamiltonian and a random choice of initial deviation vectors, we expect the GALI indices to behave as

$$\text{GALI}_2(t) \propto \text{constant}, \;\; \text{GALI}_3(t) \propto \frac{1}{t^2}, \;\; \text{GALI}_4(t) \propto \frac{1}{t^4}. \tag{34}$$

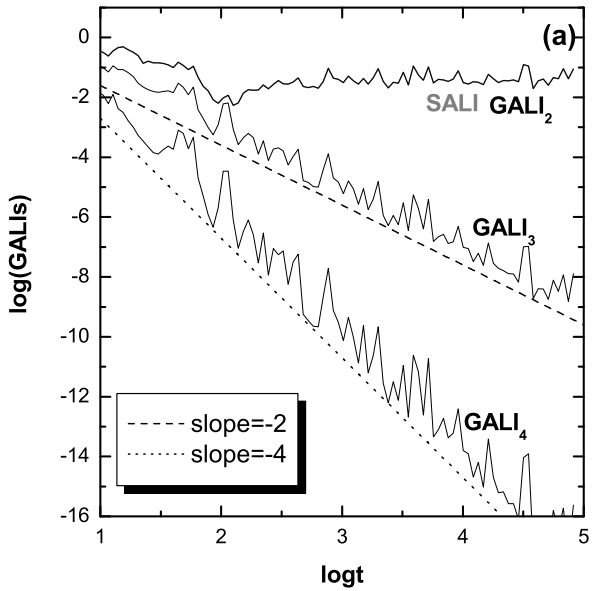

Figure 12: Time evolution of SALI (gray curves), GALI_2, GALI_3 and GALI_4 for an ordered orbit. Note that the curves of SALI and GALI_2 are very close to each other and thus cannot be distinguished. Dashed lines corresponding to particular power laws are also plotted.

Charting regular and chaotic domains in phase space

Consider, for example, GALI$_4$, for which GALI$_4 \propto e^{-4\sigma_1 t}$ for chaotic orbits and GALI$_4 \propto 1/t^4$ for ordered ones.

In general, the time needed for the index to become zero is much larger for ordered orbits. So, instead of simply registering the value of the index, let us record the time, t_{th}, needed for GALI$_4$ to reach a very small threshold, e. g. 10^{-12}, and color each grid point according to the value of t_{th}.

The outcome of this procedure for the 2D Hénon–Heiles system is presented in the next figure:

Figure 13: Each orbit is integrated up to $t = 500$ units and if the value of GALI$_4$ at the end of the integration is larger than 10^{-12}, the corresponding grid point is colored by the light gray color used for $t_{th} \geq 400$. At the border between them we find points having intermediate values of t_{th} which belong to the so – called 'sticky' chaotic regions.

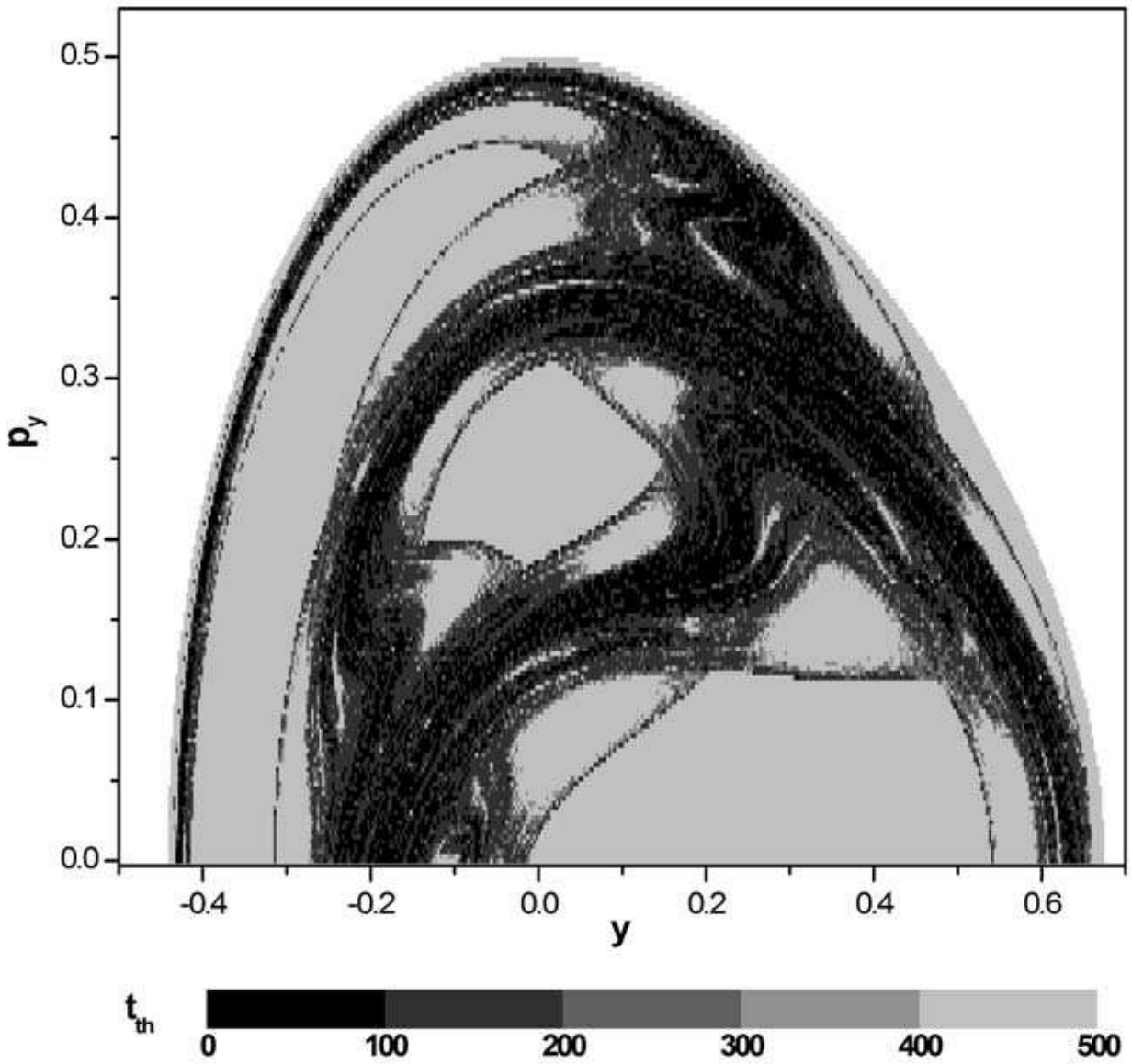
0.5
0.4
0.3
0.2
0.1
0.0
p_y
-0.4
-0.2
0.0
0.2
0.4
0.6
y
t_{th}
0
100
200
300
400
500

A 3D Hamiltonian system

Let us now study the behavior of the GALIs in the case of the 3D Hamiltonian (**??**). The initial conditions of the orbits of this system are defined by assigning arbitrary values to the positions q_1, q_2, q_3, as well as the so–called 'harmonic energies' E_1, E_2, E_3 related to the momenta through $p_i = \sqrt{\frac{2E_i}{\omega_i}}$, $i = 1, 2, 3$.

Chaotic orbits of 3D Hamiltonian systems generally have two positive Lyapunov exponents, σ_1 and σ_2, while $\sigma_3 = 0$. So, for approximating the behavior of GALIs according to (**??**), both σ_1 and σ_2 are needed. In particular, (**??**) gives

$$\begin{gathered} \text{GALI}_2(t) \propto e^{-(\sigma_1-\sigma_2)t}, \;\; \text{GALI}_3(t) \propto e^{-(2\sigma_1-\sigma_2)t}, \;\; \text{GALI}_4(t) \propto e^{-(3\sigma_1-\sigma_2)t}, \\ \text{GALI}_5(t) \propto e^{-4\sigma_1 t}, \;\; \text{GALI}_6(t) \propto e^{-6\sigma_1 t}. \end{gathered} \tag{35}$$

Let us consider the chaotic orbit with initial conditions $q_1 = q_2 = q_3 = 0$, $E_1 = E_2 = E_3 = 0.03$ of the 3D system (**??**) and compute σ_1, σ_2 for this orbit. For $t \approx 10^5$ we find $\sigma_1 \approx 0.03$ and $\sigma_2 \approx 0.008$. Using these values as good approximations of σ_1, σ_2 we see that the slopes of all GALIs are well reproduced by the analytical formulas.

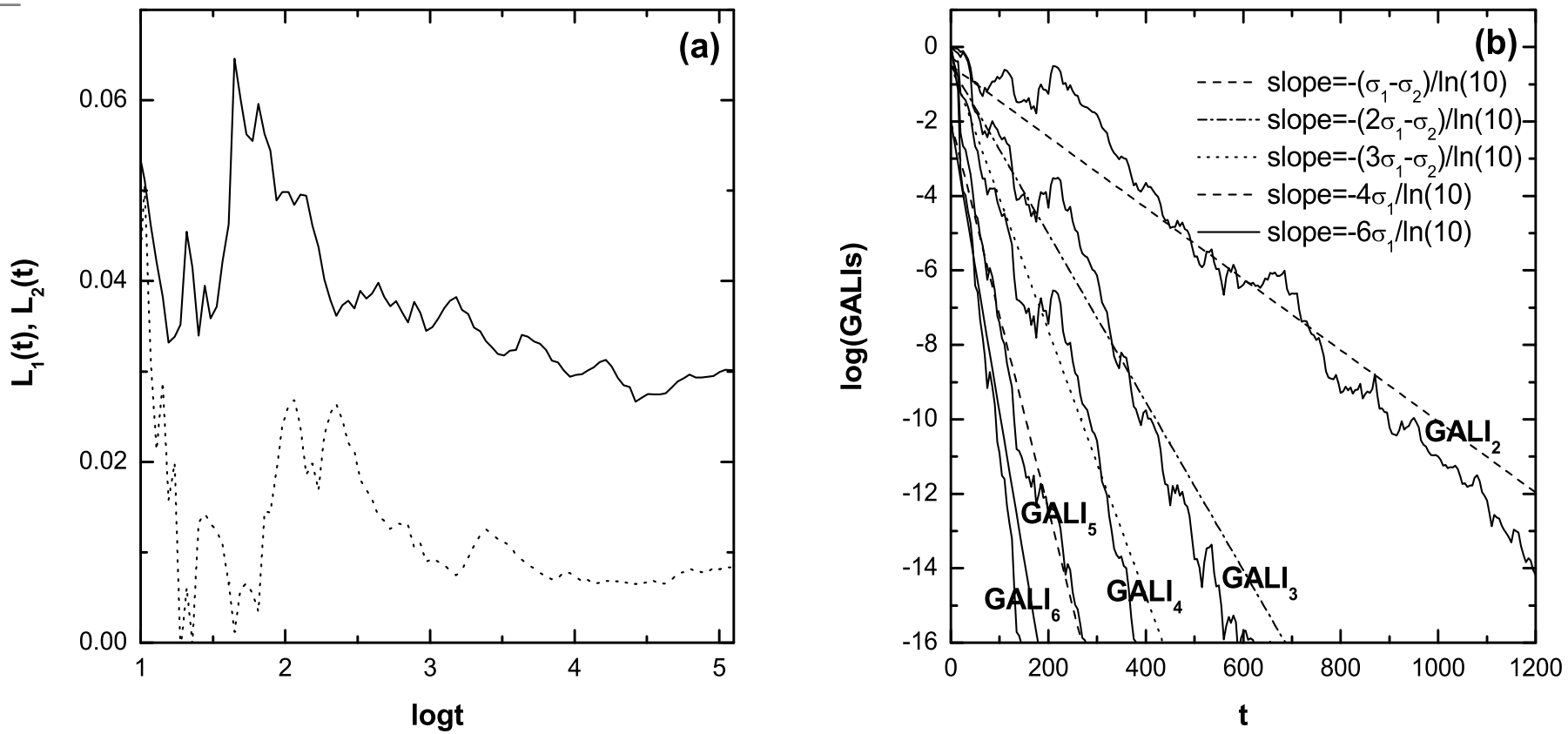

Figure 14: (a) The evolution of $L_1(t)$, $L_2(t)$ for the chaotic orbit of the 3D system. (b) The evolution of GALI$_k$ with $k = 2, \ldots, 6$. The plotted lines correspond to functions proportional to $e^{-(\sigma_1-\sigma_2)t}$, $e^{-(2\sigma_1-\sigma_2)t}$, $e^{-(3\sigma_1-\sigma_2)t}$, $e^{-4\sigma_1 t}$ and $e^{-6\sigma_1 t}$ for $\sigma_1 = 0.03$, $\sigma_2 = 0.008$.

Next, we consider the case of ordered orbits in our 3D Hamiltonian system. In general, the GALIs should behave as: $\text{GALI}_2(t) \propto$ constant, $\text{GALI}_3(t) \propto$ constant, $\text{GALI}_4(t) \propto \frac{1}{t^2}$, $\text{GALI}_5(t) \propto \frac{1}{t^4}$, $\text{GALI}_6(t) \propto \frac{1}{t^6}$.

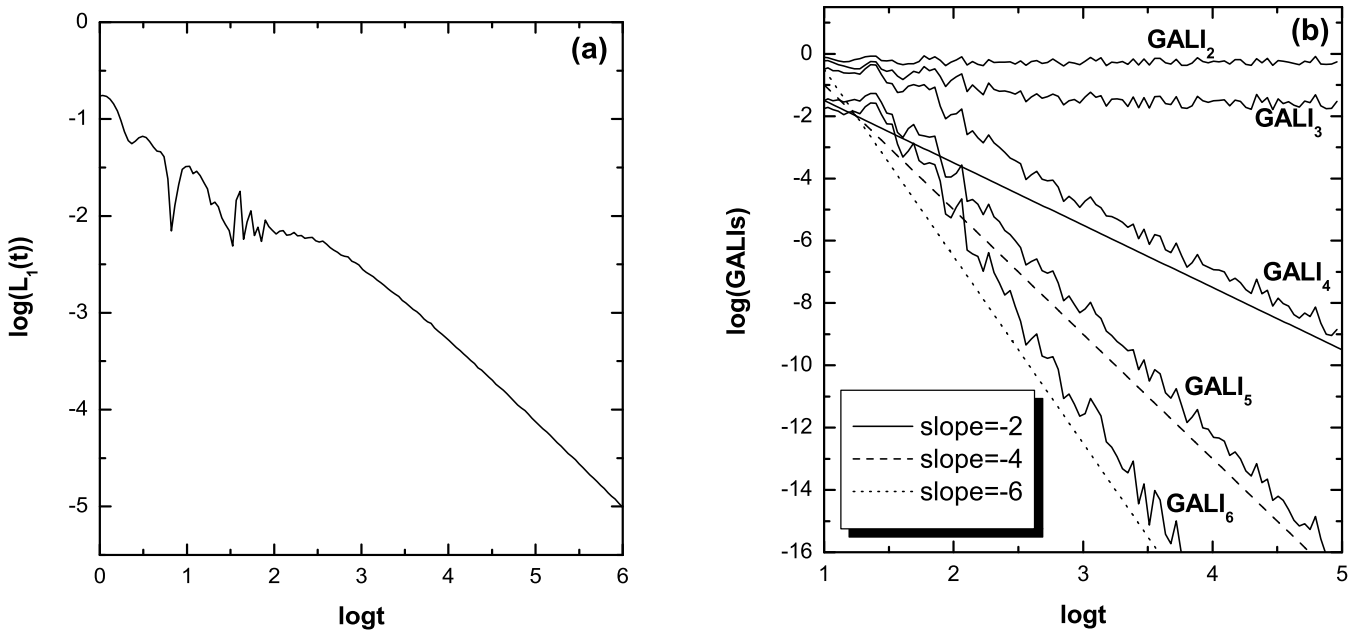

Figure 15: (a) $L_1(t)$ for the ordered orbit of the 3D system and (b) The GALI_k with $k = 2, \ldots, 6$ of the same orbit. The dashed lines are the slopes of $\frac{1}{t^2}$, $\frac{1}{t^4}$ and $\frac{1}{t^6}$.

Using GALI$_3$ instead of SALI, we gain considerably in CPU time for chaotic orbits, while we lose for ordered orbits. Thus, the efficiency of GALI$_3$

A) depends on the **percentage of phase space occupied by chaotic orbits** (if all orbits are ordered GALI$_3$ requires more CPU time than SALI).

B) However, it also depends on the **choice of the final time**, up to which each orbit is integrated.

As an example, let us integrate, up to $t = 1000$ time units, all orbits whose initial conditions lie on a dense grid in the subspace $q_3 = p_3 = 0$, $p_2 \geq 0$ of a 4–dimensional PSS, with $q_1 = 0$ of the 3D system (**??**), attributing to each grid point a color according to the value of GALI$_3$ at the end of the integration. If GALI$_3$ of an orbit becomes less that 10^{-8} for $t < 1000$ the evolution of the orbit is stopped, its GALI$_3$ value is registered and the orbit is characterized as chaotic. The outcome of this experiment is presented in the figure below, where we have projected on the p_2, q_2 plane all orbit points corresponding to $q_1 = 0$.

We find that 77% of the orbits of figure **??** are characterized as chaotic, having GALI$_3 < 10^{-8}$. In order to have the same percentage of orbits identified as chaotic using SALI (i. e. having SALI $< 10^{-8}$) the same experiment has to be carried out for $t = 2000$ units, requiring 53% more CPU time.

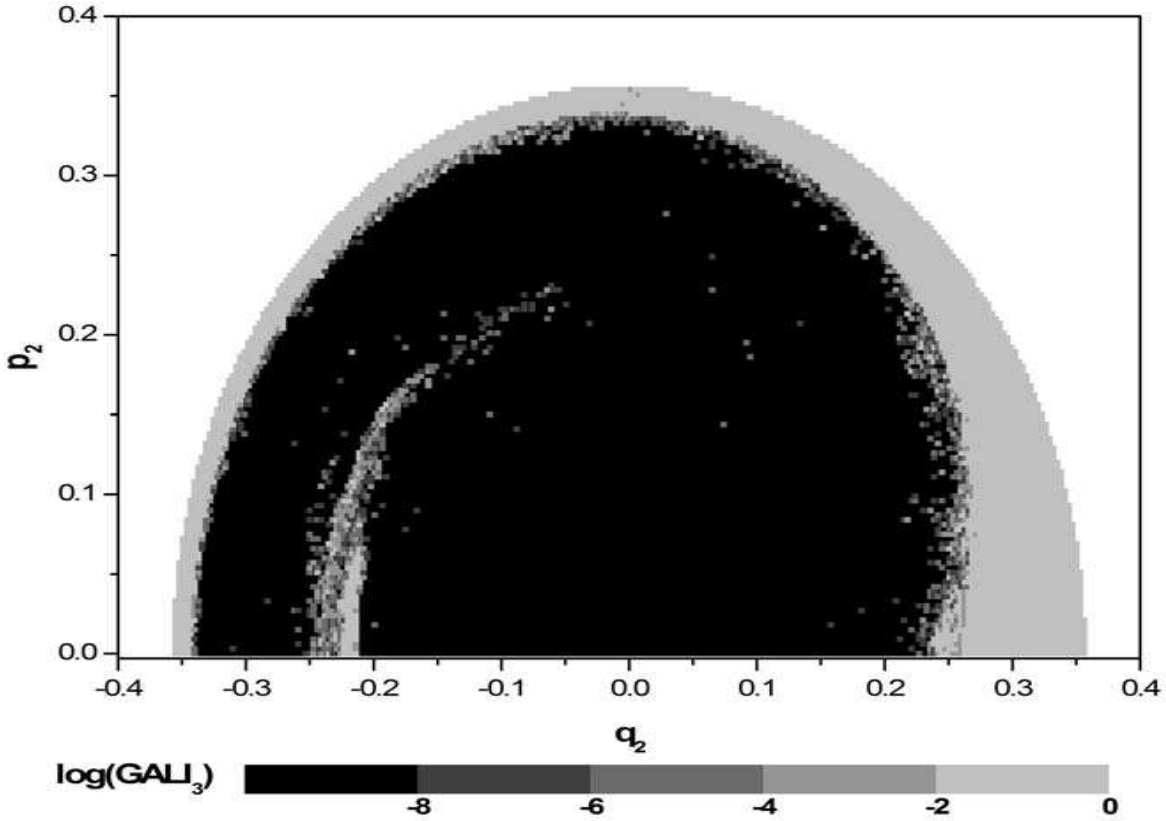

Dimensionality of Tori and Weak Diffusion

In their famous paper in 1955, Fermi, Pasta and Ulam studied energy transport in one – dimensional lattices, like the so – called β – FPU lattice described by the Hamiltonian

$$H = \frac{1}{2}\sum_{j=1}^{N} \dot{x}_j^2 + \sum_{j=0}^{N}\left(\frac{1}{2}(x_{j+1}-x_j)^2 + \frac{1}{4}\beta(x_{j+1}-x_j)^4\right) = E \tag{36}$$

When β is small, the dynamics can described by the linear normal modes

$$Q_k = \sqrt{\frac{2}{N+1}}\sum_{i=1}^{N} q_i \sin\frac{ki\pi}{N+1}, \qquad P_k = \dot{Q}_k \tag{37}$$

with energies and ("phonon") frequencies

$$E_k = \frac{1}{2}\left[P_k^2 + {\omega_k}^2 Q_k^2\right], \;\; \omega_k = 2\sin\frac{k\pi}{2(N+1)} \tag{38}$$

Fermi, Pasta and Ulam observed that, for low values of E, if the initial conditions are chosen such that one or more of the **low k - modes** ($k = 1, 2, 3, ..$) are excited, one observes the famous **FPU recurrences**!

This means that the energy returns periodically to the initial state, instead of leading to energy sharing and equipartition as expected from Statistical Mechanics. Let us see what the GALI$_k$ give when only the $k = 1$ and $k = 3$ modes modes are excited:

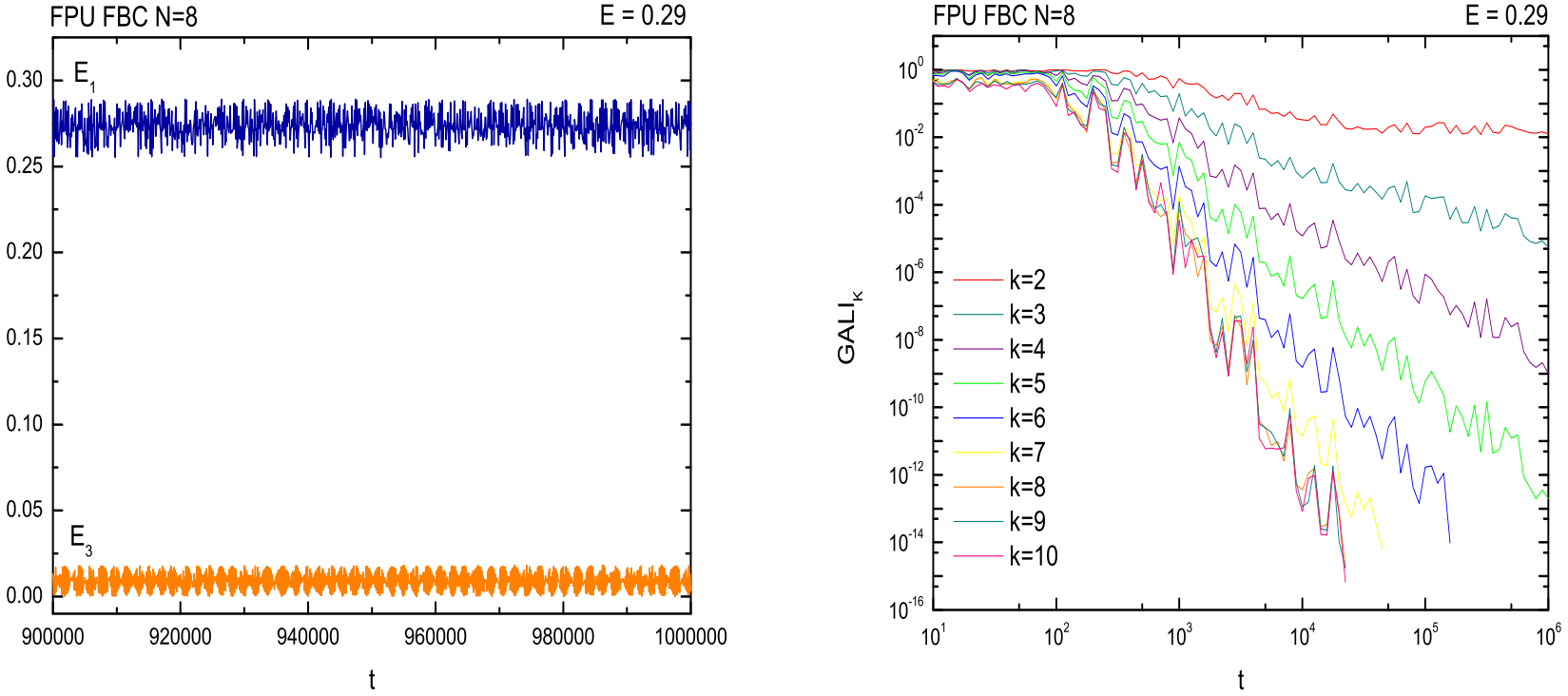

Figure 16: FPU with 8 particles:(a) Only the E_1 and E_3 modes are excited and the torus is 2-dimensional, since (b) only GALI$_2$=const. and all other GALI$_k$ decay by power laws.

Next we start by putting all the energy in the 4 modes $k = 1, 3, 5, 7$ and observe that the motion lies on a 4–dimensional torus

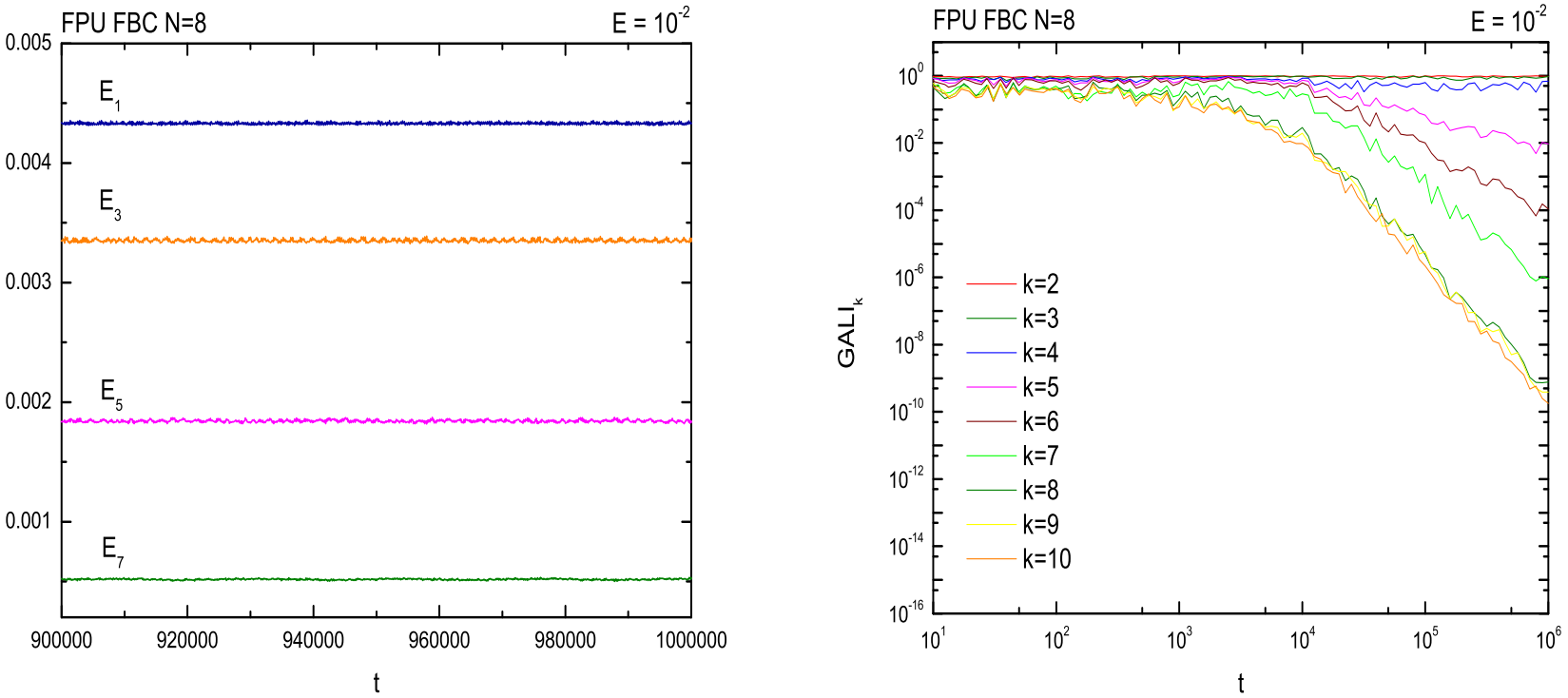

Figure 17: FPU with 8 particles:(a) When the E_1, E_3, E_5 and E_7 modes are excited the torus is 4-dimensional and (b) only the GALI$_k$=const. for $k = 2, 3, 4$, while all others, with $k = 5, \ldots, 10$ decay by power laws.

Finally we may put all energy in 8 modes and obtain a generic 8–dimensional torus:

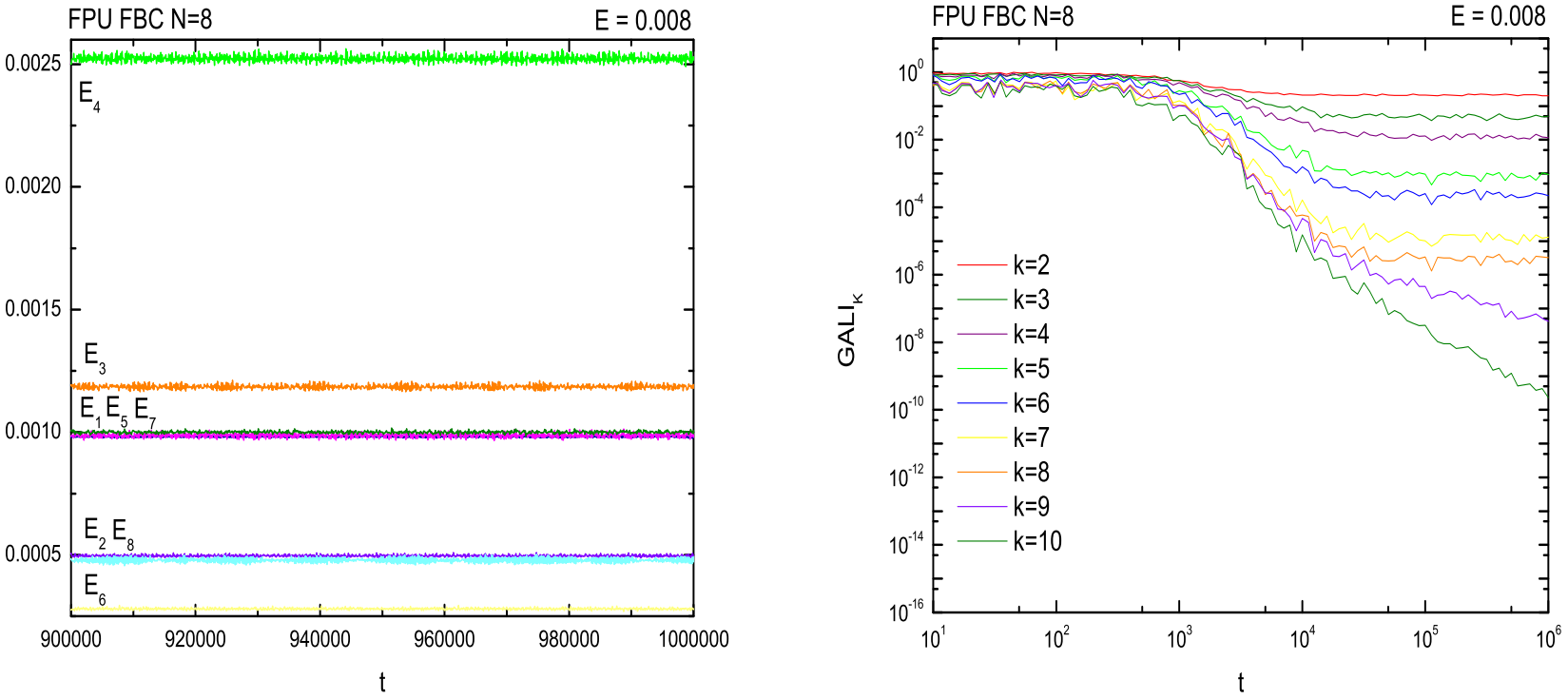

Figure 18: FPU with 8 particles:(a) When 8 modes, $k = 1, 2, ..., 8$, are excited the torus is 8-dimensional and (b) GALI$_k$=const.,for $k = 2, \ldots, 8$, while the other two with $k = 9, 10$ decay by power laws.

Predicting the onset of weak diffusion

For initial conditions **slightly off a torus** leading to slow diffusive motion away from quasiperiodicity $GALI_2$ (or SALI) predicts it quickly by falling to zero exponentially:

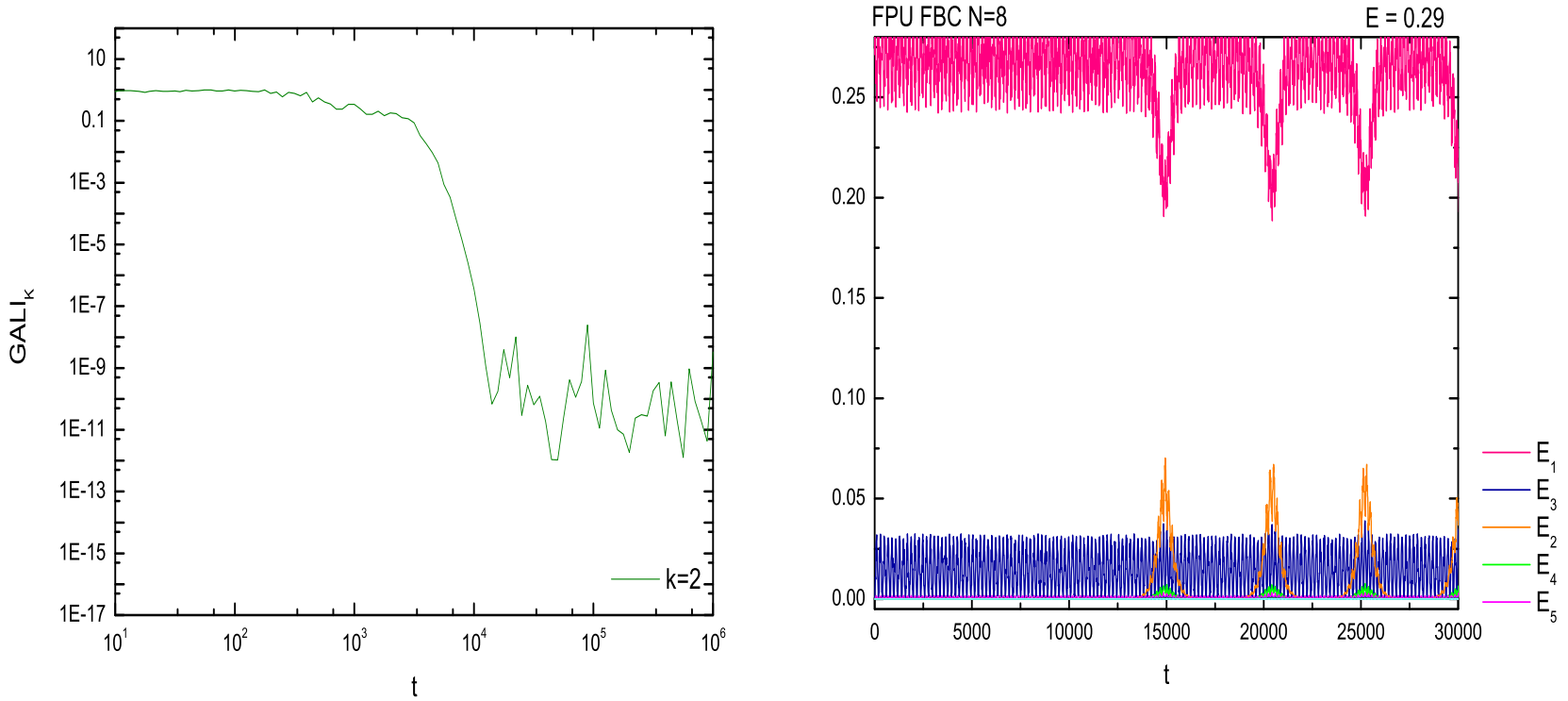

Figure 19: FPU with 8 particles:(a) The evolution of $GALI_2$ shows already at $t \approx 500$ that the orbit diffuses away from the torus and is not quasiperiodic. (b) This becomes visible in the oscillations **much later**, when the recurrences break down at $t \approx 14000$.

Quasiperiodic Breathers and their Breakdown

Finally we study a quartic Hamiltonian lattice with on site quartic potential and no linear dispersion, described by the Hamiltonian

$$H_{NL} = \frac{1}{2}\sum_{i=1}^{N} p_i^2 + \sum_{i=1}^{N}\left[\frac{1}{2}(q_{i+1}-q_i)^4 + \frac{1}{2}q_i^2(1-\epsilon cos(\omega_d t)) - \frac{1}{4}q_i^4\right] \qquad (39)$$

with fixed boundary conditions, i.e. $q_0 = q_N = p_0 = p_N = 0$. We select parameter values at which we know that the Hamiltonian (**??**) has a stable **discrete breather**.

Now, around this (periodic) breather, due to the **absence of quadratic nearest neighbor interactions**–and hence no linear spectrum to generate resonances–**quasiperiodic breathers** exist. GALI$_2$ oscillates about a constant and thus identifies the presence of a torus. And since **all higher order** GALI$_k$, with $k > 2$, decay the torus is 2–dimensional!

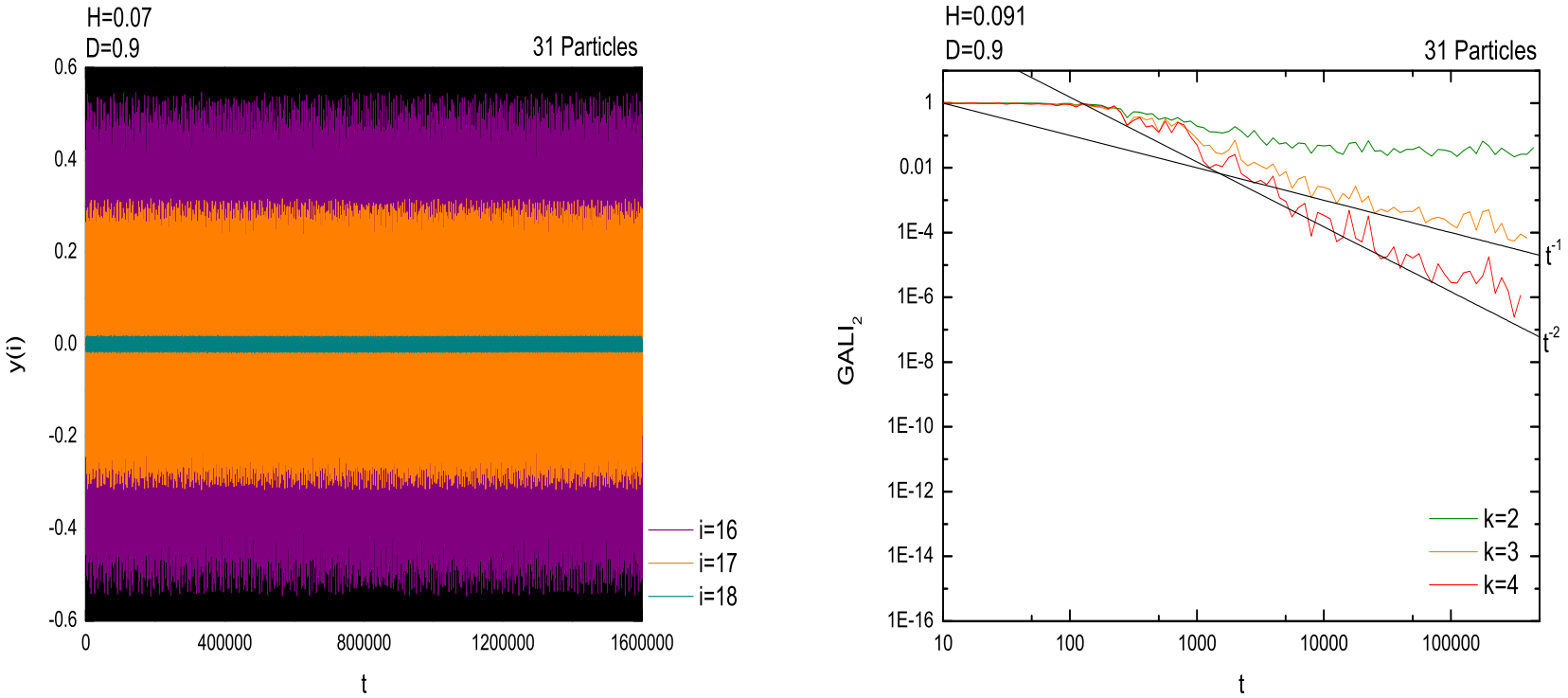

Figure 20:(a) The oscillations of the central three particles of this with $N = 31$ particles do **not break down**, forming a quasiperiodic breather. (b) The corresponding torus is 2–dimensional, as evidenced by the fact that only GALI_2 remains nearly constant, while all other GALI_k, with $k > 2$ decrease by power laws.

However, at initial conditions further away from the periodic breather, GALI_2 predicts slow diffusion by falling to zero exponentially:

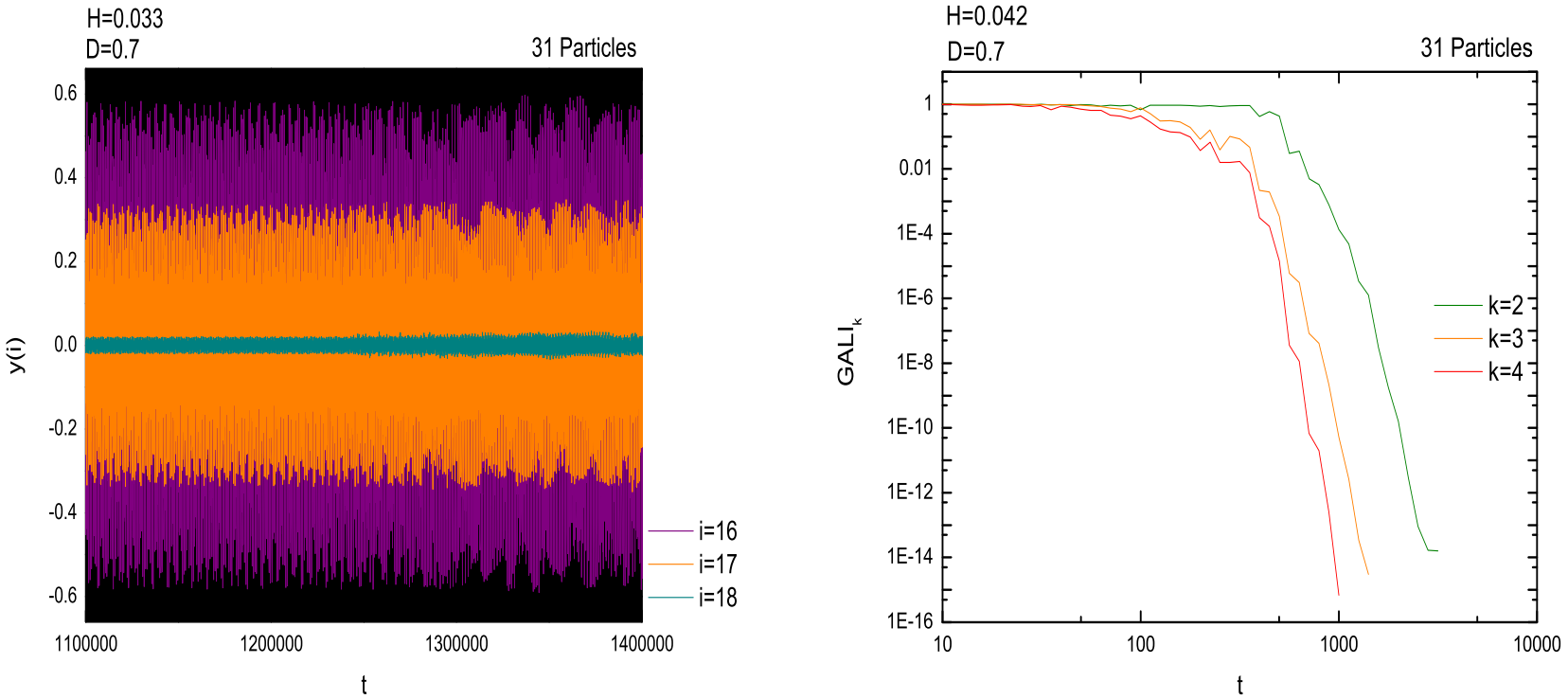

Figure 21:(a) The oscillations of the central particles of (**??**) with $N = 31$, **appear quasiperiodic** for very long times. (b) The solution, however, is **not on a torus** and diffuses slowly away, since even GALI_2 decays exponentially after about $t = 5000$.

Conclusions

1) Generalizing the SALI method, we introduced the Generalized Alignment Indices, GALI$_k$. GALI$_k$ is the 'norm' of the 'exterior' or wedge product of k normalized deviation vectors and hence represents the 'volume' of a parallelepiped having as edges $k > 2$ initially independent deviation vectors.

We have shown that for chaotic orbits:

$$\text{GALI}_k(t) \propto e^{-[(\sigma_1-\sigma_2)+(\sigma_1-\sigma_3)+\cdots+(\sigma_1-\sigma_k)]t} . \tag{40}$$

while for ordered ones:

$$\text{GALI}_k(t) \sim \begin{cases} \text{constant} & \text{if } 2 \leq k \leq s \\ \frac{1}{t^{k-s}} & \text{if } s < k \leq 2N-s \\ \frac{1}{t^{2(k-N)}} & \text{if } 2N-s < k \leq 2N \end{cases} . \tag{41}$$

where s is the dimension of the torus and no deviation vectors are initially tangent to the torus.

2) The GALI$_k$s can be successfully applied to:

a) Distinguish very rapidly **chaotic orbits**, for $2 \leq k \leq N$, **from ordered orbits** (GALI$_k$ decays exponentially or fluctuates around a constant)

b) Determine from the GALI$_k$ power law decays the **dimensionality** $d \leq N$ **of the subspace of ordered motion**, identifying **low - dimensional** tori

c) Locate initial conditions leading to **very slow diffusion** of the orbits toward a larger chaotic "sea", near nonlinear normal modes of the FPU lattice and quasiperiodic breathers

c) Efficiently **chart large domains of phase space**, identifying various degrees of order and chaos, by different behaviors of the indices.

d) Obtain analogous results also for $2N$–dimensional **symplectic maps.**

References

1. Skokos, Ch. [2001], “Alignment Indices: A New, Simple Method for Determining the Ordered or Chaotic Nature of Orbits", *J. Phys. A*, **34**, pp. 10029 – 10043.
2. Skokos, Ch., Antonopoulos, Ch., Bountis, T. C. and Vrahatis, M. N. [2003], “How does the Smaller Alignment Index (SALI) Distinguish Order from Chaos?", *Prog. Theor. Phys. Supp.*, **150**, pp. 439 – 443
3. Skokos, Ch., Antonopoulos, Ch., Bountis, T. C. and Vrahatis, M. N. [2004], “Detecting Order and Chaos in Hamiltonian Systems by the SALI Method", *J. Phys. A*, **37**, pp. 6269 – 6284.
4. Antonopoulos, Ch., Bountis, T. C. and Skokos, Ch., [2006], “Chaotic Dynamics of N–Degree–of–Freedom Hamiltonian Systems”, International Journal of Bifurcation and Chaos, vol.**16**(6), 1777-1793 , June 2006.
5. Antonopoulos, Ch. and Bountis, T., [2006], “Stability of Simple Periodic Orbits and Chaos in an FPU Lattice”, PRE**73**, 056206, 1-8 (2006).
6. T. Bountis, "Stability of Motion: From Lyapunov to N - Degree of Freedom Hamiltonian Systems", [2006], "Nonlinear Phenomena and Complex Systems", vol. **9**(3) ,209 -239, 2006.
7. Skokos, Ch., Bountis, T. and Antonopoulos, Ch. [2007], “Geometrical properties of local dynamics in Hamiltonian systems: the Generalized Alignment Index (GALI) method”, Physica D **231**, 30.